CORROSION SCIENCE AND TECHNOLOGY, Vol.31, No.6(2002), pp.432~437

Effects of Mo on the Structure and Semiconducting Properties of Passive Film Formed on 18Cr-8Ni Stainless Steels

Erwan Le Roy, EunAe Cho*, Heesan Kim, and HyukSang Kwon**

Dept. of Materials Science and Engineering, Korea Advanced Institute of Science and Technology
373-1, Kusong-dong, Yusong-gu, Taejon 305-701, KOREA
**Fuel Cell Research Center, Korea Institute of Science and Technology*
P.O.BOX 131, CheongRyang, Seoul, Korea, 130-650
***Stainless steel gr. POSCO Research Laboratories*
Pohang P.O. Box 36, 1 Geodong-dong, Nam-gu, Pohang-shi, 790-785, Korea

The influences of Mo on the structure and semiconducting properties of the passive films formed on 18Cr-8Ni stainless steels (SSs) have been examined by photo-electrochemical spectroscopy (PES) and atomic force microscopy (AFM). The photocurrent spectra for the passive films formed on 18Cr-8Ni and 18Cr-8Ni-4Mo SSs could be resolved into two component spectra, each of which was generated respectively by the d-d and the p-d electronic transitions occurring in the outer iron rich layer consisting of γ-Fe_2O_3 containing Cr^{+3}, and exhibiting n-type semiconducting behavior. The first photocurrent component associated with the d-d transition exhibited a band gap energy (E_g) of 3.0 eV with a photocurrent peak at 3.9 eV irrespective of the Mo addition, whereas the second one associated with the p-d transition showed E_g between 2.9 and 3.2 eV with a photocurrent peak at 4.2~4.5 eV. The addition of 4Mo to 18Cr-8Ni SS shifted the photocurrent peak of the second component from 4.2 to 4.5 eV, resulting from the Mo-induced Cr-enrichment in the passive film. Further, Mo alloyed with 18Cr-8Ni SS made the passive film structurally more amorphous and chemically more homogeneous when compared in terms of the disorder energy based on the Dunstan theory and the AFM topography on the passive films of on the two alloys.

Keywords : *photoelectrochemical spectroscopy, passive film, molybdenum, stainless steel, semiconducting properties.*

1. Introduction

It is well documented that the addition of Molybdenum (Mo) increases the resistance to pitting and crevice corrosion of SSs.[1-3] This is primarily due to the fact that Mo improves the stability of the passive film on SSs as confirmed by the electrochemical responses such as a reduction in the critical anodic current density, an increase in the passive range, a decrease in both the passive current density and the transpassive current density.[4]

Many researchers have tried to examine effects of Mo on the structure and composition of passive film on SSs using ex-situ techniques such as auger electron spectroscopy and X-ray photoelectron spectroscopy.[5-8] AES(Auger electron spectroscopy) depth concentration profiles for the passive film on SS showed that the passive film consisted of two layers, one of which, Cr rich layer, was placed at metal side and the other of which, Fe-rich layer, was placed at the solution side.[9] It was reported that an addition of small amount of Mo to Fe-Cr SSs increased both the chromium concentration at the film side of inner film/metal interface[8-11] and also the ratio of Cr_2O_3 oxide phase to CrOOH or $Cr(OH)_3$ hydroxide phase[10),12)]
It is well known that passive film formed on SSs has an amorphous structure due to an excellent bond flexibility of Cr, and that the amorphous degree of the passive film on SSs is increased with Cr content. The passive film on SS was also reported to have a locally crystalline structure.[13] However, the effects of Mo on the amorphous degree of passive film on SS have not yet been clarified. Most of the results on the passive film of SSs, mentioned above, were obtained by ex-situ techniques, which may not reveal the real aspects of the structure and composition of the passive film formed on SS since the nature of passive film is likely to be changed when removed from solution for an ex-situ examination. PES is a powerful in-situ technique for characterizing electronic and/or optical properties of passive film on SS, and has been

developed on the basis that passive film on SS exhibits semiconducting characteristics. Although Mo as an alloying element affects significantly the composition and structure of the passive film on SS, the influences of Mo on the photoelectrochemical response of the passive film on SS have been rarely studied.

The research objective of the present work is to examine the effects of Mo on the electronic properties of the passive film on austenitic SS by PES, with focussing on the Mo effects on the structural and chemical homogeneity of passive film.

2. Experimental procedures

Fe-18Cr-8Ni and Fe-18Cr-8Ni-4Mo were made by vacuum arc melting and then cast in a form of button. The cast was homogenized for 100 min at 1200 ℃, and then hot rolled into a 3 mm thick plate. Specimens were prepared by cold rolling the hot rolled plates into 1.5 mm thick sheets and solution annealing for 20 minutes at 1050 ℃, followed by water quenching. The specimens were mounted in an epoxy and sealed by silicone with an area of 10 mm^2, which was necessary to reduce the back current for the photocurrent measurement, and polished with SiC paper to #2000 grit. The solution used for all the experiments was a pH 8.5 buffer solution prepared by mixing 0.2 M boric acid and 0.05 M citric acid with 0.1 M tertiary sodium phosphate solution.[14] Specimens were cathodically cleaned for 10 min at -1.0 V in the solution to remove the air-formed film before potentiostatically forming passive film. All the experiments were performed at room temperature. All the potentials were referred to the saturated calomel electrode (SCE). The potentiodynamic polarization response for the specimens was monitored under a scanning rate of 0.5 mV/s using a conventional polarization cell.

A conventional three electrode cell of 1 L-multineck flask with a quartz window as a photon inlet was used for the measurement of photocurrent for the passive film that has been formed potentiostatically for 24 hours. A 300W Xenon arc lamp combined with a scanning digital monochromator was used to impose a monochromatic illumination to the working electrode. The monochromator was controlled at a scanning rate of 1nm/s by stepping motor, which made it possible to provide automatically the monochromatic photons with 200 to 800 nm wave length to the working electrode. To increase the photon flux, white light from the Xe lamp was focused to the light inlet using two auxiliary focusing lenses. For AFM observation on the surface of passive film, the samples were polished to 1 μm in order to avoid scratch visualization on the scan range (5 μm^2). Passive film grown at 200 mV_{SCE} were rinsed in acetone, and then directly observed with non-contact AFM equipment.

3. Results and discussion

3.1 Potentiodynamic polarization response

Fig. 1 shows potentiodynamic curves of 18Cr-8Ni and 18Cr-8Ni-4Mo SSs in the pH 8.5 buffer solution. Evidently, the current density of 18Cr-8Ni-4Mo SS is slightly lower than that of the alloy without Mo, exhibiting a formation of more stable passive film on the alloy with 4Mo. The current density increased slightly at potentials above 0.5 V_{SCE} due to Cr transpassivation. For photocurrent measurements, XPS, and AFM, passive film was potentiostatically formed on the two alloys at a stable passive potential of 200 mV_{SCE}.

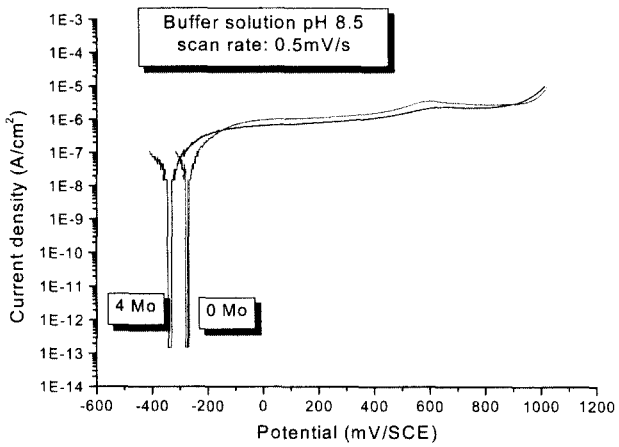

Fig. 1. Potentiodynamic polarization responses for Fe-18Cr-8Ni and Fe-18Cr-8Ni-4Mo SSs in the pH 8.5 buffer solution at 25 ℃.

3.2 Photocurrent electrochemical spectroscopy

In order to examine the electronic and structural properties of the passive film, photocurrent spectra for the passive film on the two SSs were measured as a function of photon energy. Fig. 2 and 3 shows photocurrent spectra for the passive films formed on 18Cr-8Ni and 18Cr-8Ni-4Mo, at 200 mV_{SCE}. Anodic photocurrent for the two alloys reflects that the passive films formed on the two alloys are an n-type semiconductor. Each photocurrent spectrum appears to be composed of 2 spectra, each of which is associated with a specific electronic transition with specific band gap energy. By assuming that the each photocurrent spectrum follows a gaussian distribution, the photocurrent spectra for the passive film on the alloys can

be resolved into two components, as shown in Fig. 2 and 3. The photocurrent spectrum for the passive film on 18Cr-8Ni SS was resolved into two components with photocurrent peak at 3.85 and 4.2 eV, whereas that for the alloy with 4Mo with photocurrent peaks at 3.9 and 4.5 eV. Compared with the photocurrent spectra for the passive film formed on Fe under the same condition as employed in this study, the photocurrent spectra for the passive films on 18Cr-8Ni SSs resembled for Fe,[15] reflecting that the photocurrent behavior of the passive film on 18Cr-8Ni SS is dominated by the outer Fe-rich layer of the passive film rather than Cr-rich inner layer. It was reported in the previous study[15] that the first and the second photocurrent peak at 3.9 and 4.3 eV were generated respectively by the d-d transition involving an electronic transition from Fe^{3+} band to Fe^{2+} band and the p-d transition involving the electronic transition from the valence band (O-2p) to the conduction band (Fe-3d) that occur in γ-Fe_2O_3 of the passive film on Fe.

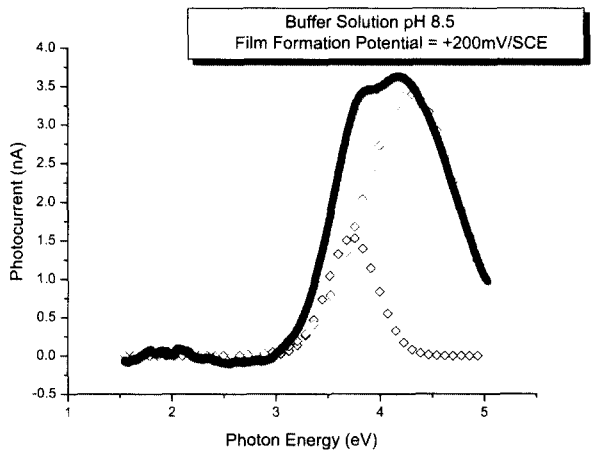

Fig. 2. Photocurrent spectra for the passive film formed on Fe-18Ni-8Cr at + 200 mV/SCE in deaerated pH 8.5 buffer solution, and its resolution into its component spectrum.

The normalized photocurrent spectra for the passive films formed on the two alloys were compared in Fig. 4. It is noted that the first peak generated by an electronic transition between Fe ions significantly decreased by the addition of Mo to 18Cr-8Ni, which could be attributed to the fact that the passive film on the alloy with 4 Mo contains less Fe ions. Another point to be noted is the shift of the second peak to high photon energy region; 4.2 eV for 18Cr-8Ni, and 4.5 eV for 18Cr-8Ni-4Mo. Analytical studies have shown that passive film on SSs contains Cr ions as well as Fe ions.[5-8] Thus, Cr ions presumably participating in the p-d transition may shift the current peak to high photon energy region because Cr has higher bonding energy with oxygen than does Fe. These results imply that the passive film on Fe-18Cr-8Ni-4Mo contains higher concentration of Cr ions in the passive film than Fe-18Cr-8Ni, thereby resulting in the shift of the photocurrent peak.

In order to examine the origin for the shift of the photocurrent peak to high photon energy region, we immersed 18Cr-8Ni SS in a 50 vol. % nitric acid solution for one hour to increase the Cr content in the passive film,[16] and then measured the photocurrent at 200 mV_{SCE} in the pH 8.5 solution. Fig. 5 compares the normalized photocurrent spectra for the passive films formed on the alloy with and without pre-acid treatment. It is significant that the photocurrent spectrum for the alloy subjected to the pre-acid

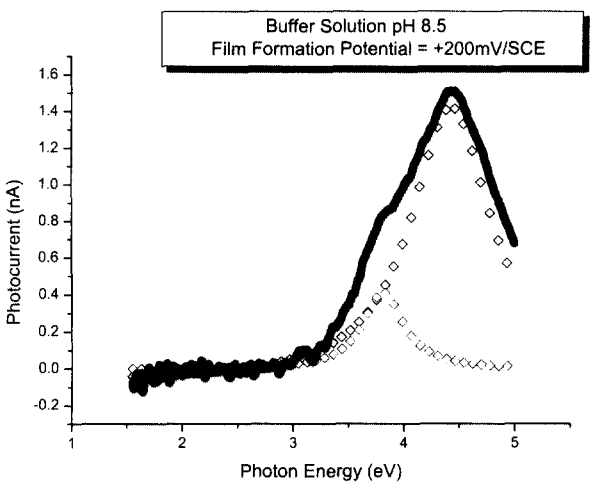

Fig. 3. Photocurrent spectra for the passive film formed on Fe-18Ni-8Ni-4Mo at + 200 mV_{SCE} in deaerated pH 8.5 buffer solution, and its resolution into its component spectrum.

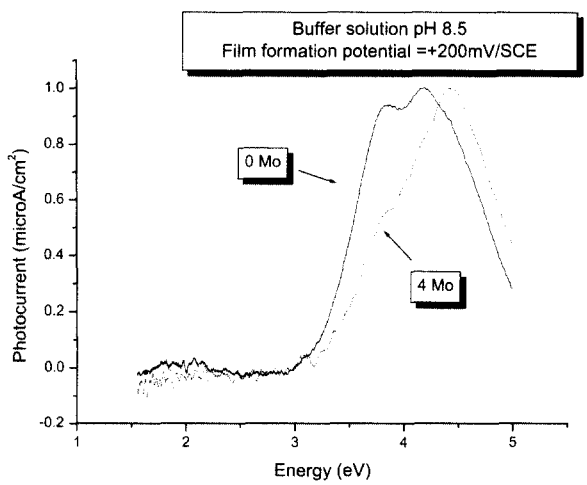

Fig. 4. Normalized photocurrent spectra for the passive films on Fe-18Cr-8Ni and Fe-18Cr-8Ni-4Mo polarized for 24 hrs. at +200mV_{SCE} in pH 8.5 buffer solution.

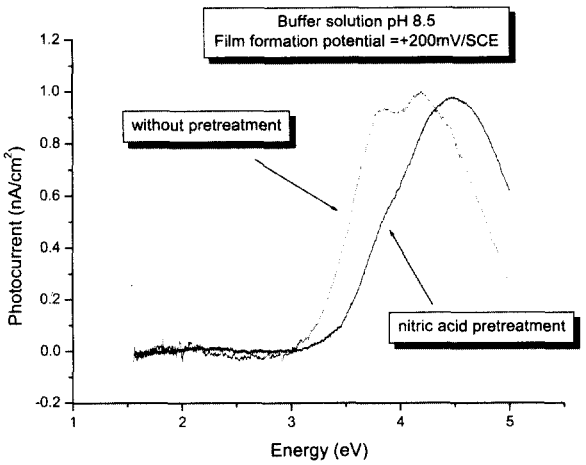

Fig. 5. Effects of pre-acid treatment on the photocurrent spectrum for the passive film on Fe-18Cr-8Ni in pH 8.5 solution; the pre-acid treatment was done by exposing the alloy to 50% HNO_3 solution for 1 hour.

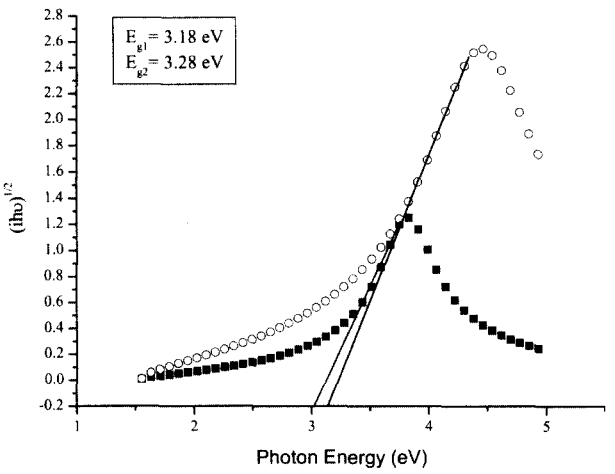

Fig. 6. Determination of the optical band gap energy for the passive film formed on Fe-18Ni-8Cr-4Mo SS at 200 mV_{SCE} in pH 8.5 buffer solution.

treatment was very similar to that for 18Cr-8Ni-4Mo SS; an appearance of two peaks at 3.9 and 4.5 eV, the decrease of the first peak intensity and the shift of the photocurrent peak to high photon energy region. Thus, the results suggest that higher Cr content in the passive film on the Mo containing alloy was responsible for the reduction in the photocurrent of the first peak as well as the shift of second peak.

3.3 Band gap energies determination

The absorption coefficient, α, of a crystalline material depends on the photon energy according to equation (1):

$$\alpha = A(h\nu - E_g)^n/h\nu \quad (1)$$

where A is a constant, and E_g the band gap energy. For crystalline semi-conductors, n depends on the electron transition type; 1/2 for direct transition, and 2 for indirect transition. However, 2 has been mostly preferred to analyze the passive film.[17] The E_g for the passive film can be determined from the $(I_{ph}h\nu)^{1/2}$ vs. $h\nu$ plot, provided that the photocurrent (i_{ph}) for the film is proportional to the absorption coefficient, and is estimated at the photon energy value where the i_{ph} equals 0.

From the each resolved photocurrent spectra for Fe-18Cr-8Ni-4Mo alloy, the E_g has been determined to be 3.00 eV and 3.16 eV respectively for the first and the second spectrum as shown in Fig. 6. The E_g for the first spectrum were 3.0eV irrespective of the Mo addition or the pre-acid treatment. This implies that the d-d transition is not affected by the Cr content in passive film.

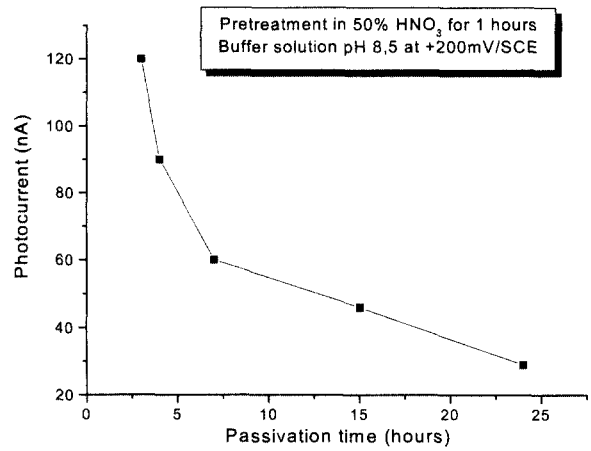

Fig. 7. Decrease in the peak photocurrent with polarization time at 200 mV_{SCE} for the passive film formed on pre-acid treated 18Cr-8Ni SS.

3.4 Effects of polarization time

Fig. 7 shows that the peak photocurrent for the pre-acid treated 18Cr-8Ni sample decreased from 120 nA to 40 nA with polarization time at 200 mV_{SCE}. The decrease in the peak current with the polarization time was also observed for the alloy without pre-acid treatment. The decrease of photocurrent with aging is thought to be due to the substitution of Cr for Fe in γ-Fe_2O_3 consisting of the outer passive layer. On the other hand, the passive film formed on Fe-18Cr-8Ni in pH 8.5 buffer solution consists of γ-Fe_2O_3 containing Cr^{3+}, which reduces intensity of photocurrent. Thus, increase in Cr content in the passive film by pre-treatment in nitric acid solution or by addition of 4Mo to Fe-18Cr-8Ni could reduce the

intensity of photocurrent.

3.5 Amorphous state of the film (Dunstan theory)

Dunstan reported that the fluctuation behavior of the E_g of a semiconductor was associated with its structural disorder,[18] and suggested a new material constant (E_o) in amorphous semiconductors that is the sum of the optical band gap (E_{og}) and the disorder energy ($1/\beta$);

$$E_o = E_{og} + 1/\beta$$

According to his model, E_o has a constant value for a crystalline semiconductor without any crystal defect by assuming that that the structural disorder of amorphous semiconductor is not influenced by a direct interaction with electronic states, but only by a microstrain field.

The disorder energy is determined by the exponential absorption tail observed below the intrinsic absorption edge in amorphous semiconductors, described by: $\alpha(h\nu) = \exp(\beta h\nu)$. The value $E_{og} = E_0\text{-}1/\beta$ represents the dependence of the E_g on the disorder. Assuming the photocurrent is proportional to the absorption coefficient, the value of β was determined to be 200 meV from the plot of ln (i_{ph}) vs. photon energy as shown in Fig. 8. The disorder energy of 200 meV corresponds to a high amorphous state.

Similarly, the average disorder energy for the passive film on18Cr-8Ni-4Mo SS materials was determined to be 3.2 eV that is about 0.07 eV higher than that for the alloy without Mo. The results suggest that the passive film formed on the alloy with 4 Mo is more amorphous or more disordered than that on the alloy without Mo.

It is well known that with an increase in the Cr content, the structure of passive film formed on SSs gets more amorphous due to a bond flexibility of Cr.[19] Thus, the increase in the average disorder energy or in the amorphous degree of the film formed on the alloy with 4 Mo appears to be associated with the Mo induced Cr enrichment in the passive film as was mentioned in the previous section based on the similarity in the photocurrent spectra for the passive films between 18Cr-8Ni-4Mo SS and the pre-acid treated 18Cr-8Ni SS.

3.6 Atomic force microscopy

In consideration of the influences of Mo on the Cr content and amorphous nature of passive film on SS, Mo alloyed in SS may also modify the topography of passive film on SS. Fig. 9 shows AFM three dimensional images on the surface of passive film grown respectively on 18Cr-8Ni and 18Cr-8Ni-4Mo alloys polarized for 24 hr at 200 mV_{SCE} in pH 8.5 buffer solution. The AFM images for the passive films demonstrated that there is a significant difference in the topographical structure of passive film between the two alloys. The surface of passive film on the alloy without Mo exhibited a large number of peaks higher than 500 A with an average roughness of 200 A, whereas that on the alloy with 4Mo showed more smooth surface with an average roughness of 87 A and all the peaks lower than 200 A.

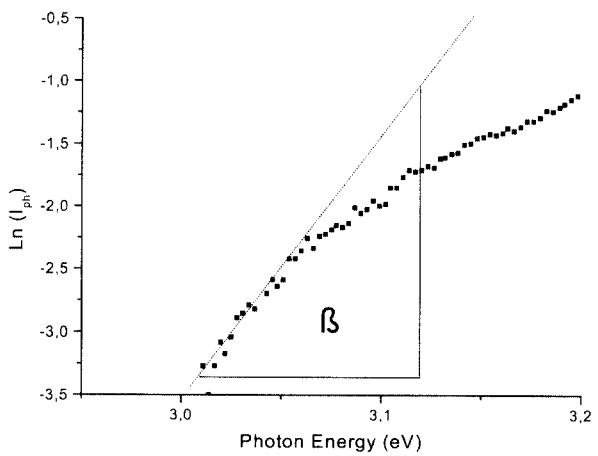

Fig. 8. Evaluation of the disorder energy from the plot of ln (i_{ph}) vs. $h\nu$ for the passive films on Fe-18Cr-8Ni polarized for 24 hrs. at +200mV_{SCE} in pH 8.5 buffer solution

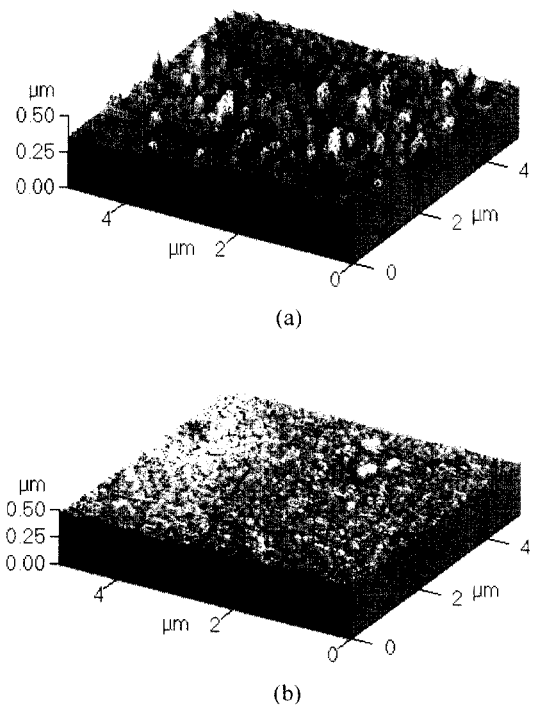

Fig. 9. Three-dimensional AFM topography for the passive films formed on 18Cr-8Ni (a) and 18Cr-8Ni-4Mo (b) alloys. The passive films were grown for 24 hr at 200mV_{SCE} in pH 8.5.buffer solution.

The high and localized peaks observed on the surface of the passive film on the alloy without Mo appears to be associated with electroactive defect sites in the film, as observed also previously on the surface of passive film iron.[20] Such electrochemically active sites might be formed due to heterogeneity in the concentration of iron in the passive film, and be susceptible to pit nucleation in a corrosive environment. On the other hand, the smooth topography of the passive formed on the alloy with 4 Mo demonstrates that Mo alloyed with SS cause the passive film to be chemically homogeneous as well as to be structurally amorphous.

4. Conclusions

1) The photocurrent spectra for the passive films formed on 18Cr-8Ni SS and 18Cr-8Ni-4Mo SS were dominated predominantly by those for the outer iron rich layer with γ-Fe_2O_3 containing Cr^{3+}, and exhibiting n-type semiconducting behavior. The photo current spectra for the passive films on both SSs could be resolved into two components of photo-current spectrum, each of which has photocurrent peaks respectively at 3.9 eV and 4.2~4.5 eV.

2) The resolved photocurrent spectrum comprising the first photocurrent peak at 3.9 eV was generated by the d-d transition from Fe^{3+} band to Fe^{2+} band, and exhibited E_g of 3.0 eV irrespective of Mo addition, while the second resolved spectrum comprising the photocurrent peak at 4.2~4.5 eV was generated by the p-d transition, and exhibited an E_g between 2.9 and 3.2 eV.

3) The shift of photo current peak to the region of high photon energy by the addition of 4 Mo to 18Cr-8Ni SS was associated with the Mo induced Cr enrichment in the passive film on SS.

4) Mo alloyed with 18Cr-8Ni SS caused the passive film to be structurally more amorphous and chemically more homogeneous when evaluated in terms of the disorder energy based on the Dunstan theory and the AFM topography for the passive films on the two alloys

Acknowlegements

The authors gratefully acknowledge the financial support from Korea Science and Engineering Foundation (KOSEF) under the grant No. 995-0800-006-2. This work was partly supported by the Brain Korea 21 project.

References

1. P. Lacombe, B. Baroux, and G. Beranger, Les aciers Inoxydables, Les Editions de Physique, Les Ulis (1990).
2. C. Lemaitre, A.A. Moneim, R. Djoudjou, B. Baroux, and G. Beranger, *Corr. Sci.*, **34**, 1913 (1993).
3. S. Maximovitch, G. Barral, F. Le Cras, and F. Claudet, *Corros. Sci.*, **37**, 271 (1995).
4. M. A. Tullmin and F. P. A. Robinson, *Corrosion*, **48**, 569 (1992).
5. I. Olefjord, B. Brox, and U. Jelvestam, *J. Electrochem. Soc.*, **132**, 2854 (1985).
6. J. N. Wanklyn, *Corros. Sci.*, **21**, 211 (1981).
7. K. Hasimoto, K. Asami, and K. Teramoto, *Corros. Sci.*, **19**, 3 (1979).
8. K. Sugimoto and Y. Sawada, *Corros. Sci.*, **17**, 425 (1977).
9. N. E. Hakiki, Da Cumha Belo, A. M. P. Simoes, and M. G. T. S. Feirreira, *J. Electrochem. Soc.*, **145**, 3821 (1998).
10. C. R Clayton and Y. C Lu, *J. Electrochem. Soc*, **133**, 2465 (1986).
11. Y. C Lu, C. R Clayton, and A. R Brooks, *Corros. Sci.*, **29**, 863 (1989).
12. I. Olefjord and B. O Elfstrom, *Corrosion NACE*, **38**, 46 (1982).
13. P. Marcus and V. Maurice, Abstract No. 334.
14. G. J. Shugar and T. Ballinger, in *Chemical Technicians' Ready Reference Handbook*, 3rd edn, Mc Graw Hill, New York, NY, 655 (1990).
15. J. S. Kim and E. A Cho, Photo-electrochemical studies on the passive film on Fe, to be published.
16. T. Shibata, S. Fujimoto, O. Yamazaki, and T. Haruna, *Proceedings of the 11th Asia-Pacific Corrosion Control*, 36 (1999).
17. U. Stimming, *Electrochem. Acta*, **31**, 415 (1986).
18. D. J Dunstan, *J. Phys C: Solid State Phys*, **16**, L567 (1983).
19. A. G. Revesz and J. Kruger, Passivity of Metals, ed. R. P. Frankenthal and Kruger, *the electrochem. Soc.*, pp.137-155 (1978).
20. Jing Li, Dale J. Meier, *Electroanalytical Chemistry*, **454**, 53 (1998).